Accepted manuscript doi: 10.1680/jbren.22.00017

Accepted manuscript
As a service to our authors and readers, we are putting peer-reviewed accepted manuscripts (AM) online, in the Ahead of Print section of each journal web page, shortly after acceptance.

Disclaimer
The AM is yet to be copyedited and formatted in journal house style but can still be read and referenced by quoting its unique reference number, the digital object identifier (DOI). Once the AM has been typeset, an 'uncorrected proof' PDF will replace the 'accepted manuscript' PDF. These formatted articles may still be corrected by the authors. During the Production process, errors may be discovered which could affect the content, and all legal disclaimers that apply to the journal relate to these versions also.

Version of record
The final edited article will be published in PDF and HTML and will contain all author corrections and is considered the version of record. Authors wishing to reference an article published Ahead of Print should quote its DOI. When an issue becomes available, queuing Ahead of Print articles will move to that issue's Table of Contents. When the article is published in a journal issue, the full reference should be cited in addition to the DOI.

Accepted manuscript doi: 10.1680/jbren.22.00017

Submitted: 30 April 2022

Published online in 'accepted manuscript' format: 17 August 2022

Manuscript title: Application of Couple Sparse Coding in Smart Damage Detection of Truss Bridges

Authors: Milad Fallahian[1], Ehsan Ahmadi[2], Saeid Talaei[1], Faramarz Khoshnoudian[1] and Mohammad M. Kashani[3]

Affiliations: [1]Faculty of Civil Engineering, Amirkabir University of Technology, Tehran, Iran; [2]Faculty of Engineering and the Built Environment, Birmingham City University, Birmingham, UK and [3]Faculty of Engineering and Physical Sciences, University of Southampton, UK

Corresponding author: Ehsan Ahmadi, Faculty of Engineering and the Built Environment, Birmingham City University, Birmingham, UK.

E-mail: Ehsan.ahmadi@bcu.ac.uk

Accepted manuscript doi:
10.1680/jbren.22.00017

Abstract

Damage detection of bridge structures plays a crucial role in in-time maintenance of such structures, which subsequently prevents further propagation of the damage, and likely collapse of the structure. Currently, the application of machine learning algorithms are growing in smart damage detection of structures. This work focuses on application of a new machine learning algorithm to identify the location and severity of damage in truss bridges. Frequency Response Functions (FRFs) are used as damage features, and are compressed using Principal Component Analysis (PCA). Couple Sparse Coding (CSC) is adopted as a classification method to learn the relationship between the bridge damage features and its damage states. Two truss bridges are used to test the proposed method and determine its accuracy in damage detection of truss bridges. It is found that the proposed method provides a reliable detection of damage location and severity in truss bridges.

Keywords: Smart Damage Detection; Frequency Response Function (FRF); Principal Component Analysis (PCA); Couple Sparse Coding (CSC); Truss Bridges

1. Introduction

To avoid partial replacement, catastrophic structural failures, and even collapse of civil infrastructures, and make informed decisions on maintenance strategy, structural health monitoring (SHM) and damage assessment are of great importance (Avci et al., 2018). The concept of damage is often defined as the comparison between two states of the structure: undamaged and damaged states. Damage identification, localization, and severity estimations are among the main aspects of SHM (Bokaeian et al., 2021; Fallahian et al., 2022). In most practical cases, damages exhibit their presence as variations in vibrational characteristics of the structure such as natural frequencies, damping ratios, and dissipated energy (Doebling et al., 1998). This means that any remarkable difference in the vibration characteristics of a system can be attributed to a certain type of damage. Then, it is feasible to correlate each change in the vibration signature to a specific type of damage and the location of damage (Zhao et al., 2019).

Damage feature selection is one of the main important steps of any SHM system, which is generally identifying the most relevant damage indicator. Recently, a new wavelet transform-based method was developed to identify natural frequencies and damping ratios of civil structures using ambient vibrations (A.Perez-Ramirez et al., 2016). However, indirect measurement of modal characteristics causes errors, and also the completeness of modal data is not achieved in practice (Lee and Shin, 2002). Among all types of vibration responses, Frequency Response Functions (FRFs) are one of the easiest to measure in real-time, as only a small number of sensors is required (Fang et al., 2005). Moreover, various frequency-domain procedures like simple peak-picking of the natural frequencies from FRFs have been utilized for damage identification procedures (Padil et al., 2020). Unlike the modal-domain data, which are extracted from a limited range around natural frequencies, the FRF data can provide much damage information over a desired frequency range (Lee and Shin, 2002). Nevertheless, if improper frequency range is selected, the measurement errors of the FRF data may seriously affect damage detection results (Ni et al., 2006; J.A. Pereira et al., 1995). To prevent measurement errors, a new approach composed of uncertain FRFs and the bootstrap method was developed (Furukawa et al., 2006). In a different study, two FRFs of different frequency ranges were iteratively used to reduce analysis time of damaged structures for damage detection purposes (Hwang and Kim, 2004). The frequency-domain response of structures contains a large amount of information on damage existence, location and severity. Although frequency-domain damage identification methods have advantages over time-domain approaches, yet, there exist many challenges and shortages in frequency-domain techniques, which need to be resolved.

In general, there are two main approaches to SHM: (1) model-based, and (2) data-based. The model-based approach is updating a Finite Element model of the structure, based on the measured data, which identifies any deviation from undamaged state of the structure. The data-based approach uses the data from both undamaged and damaged states of the structure to establish a relationship between damage features and damaged states of the structure through machine learning methods. The Multi-Layer Perceptron (MLP) is one of the most commonly methods, that has been used in machine learning-based SHM approaches (Alexandrino et al., 2020; Tan et al., 2020; Zenzen et al., 2020). The MLP networks are able to approximate any continuous multivariate function to any degree of accuracy (Rumelhart et al., 1986; Li and Fang., 2012). Further, a back-propagation based neural network method was used to estimate damage intensities of joints in truss bridges (Mehrjoo et al., 2008). However, the method could not detect relatively small damages due to modeling deviations and measurement uncertainties, such as noise. Xu et al. (2004) used a new neural network strategy to directly identify damage features from the forced time-domain vibration responses of the structure (Xu et al., 2004).

Due to the large size of data as well as presence of measurement noise, FRFs cannot be used in Artificial Neural Networks (ANNs). So, reduction techniques such as Principal Component Analysis (PCA) were used to reduce the dimension of the data (Dackermann et al., 2013). PCA-compressed FRF data from undamaged and the damaged structures were inputted to ANNs to identify damage location and severity (Li et al., 2012). Recently, an ANN-based approach was developed to extract damage indices from the ambient vibration response of a structure (Avci et al., 2020). Furthermore, a new method based on deep neural network has proposed to identify and localize damages of building structures equipped with smart control devices (Yu et al., 2019).

Sparse Representation (SR) methods have also received much attention in SHM community. The main advantages of SR methods are interpretation of data points in a more elegant way, quick retrieval of the data, and more flexibility in data representation. Hence, SR methods have been extensively used in many pattern recognition tasks, including face recognition and object classification (Wright et al., 2009). A couple sparse coding (CSC) was developed

Accepted manuscript doi:
10.1680/jbren.22.00017

based on simple sparse coding algorithm (Zolfaghari et al., 2014). In comparison with simple sparse coding algorithm, the CSC algorithm gives a smaller estimation error. Based on combining deep neural network and sparse coding, a damage identification method was developed and experimentally verified (Fallahian et al., 2018b). The results demonstrated the robustness of the proposed method in damage detection of structures. Further, the authors investigated the application of the CSC algorithm in damage identification of frame structures (Fallahian et al., 2018a).

In aged truss bridges, ever-changing stiffness of truss members is a common and serious issue. Hence, in this study, the application of the CSC algorithm in damage detection of truss bridges is addressed. PCA-compressed FRF data are used to produce damage features as the inputs for the CSC algorithm. To investigate the efficiency and practicability of the proposed method in damage detection of truss bridges, several types of damage scenarios, including single and multiple damages, are considered in two real-life truss bridges. For multiple damage scenarios, the maximum number of damaged members are considered 4 in this study, while in previous studies, structures have not been damaged at more than two members (Bandara et al., 2014). Additionally, the measured FRF data is considered to contain high levels of noise pollution, up to 20%, compared to previous researches, as taken a maximum noise level of 10% (Bandara et al., 2014; Dackermann et al., 2013; Mehrjoo et al., 2008).

2. Proposed Damage Detection Algorithm

Figure 1 shows the damage detection algorithm proposed in this study. The data set includes FRF data and damage data (stage 1). FRF data are usually the most compact form of data obtained from vibration testing, and have appeared as one of the very promising damage features for damage detection in recent years. The FRF can be measured from an actual truss bridge or can be extracted from reliable and accurate numerical models of a truss bridge. The damage data contain location of each truss member (member number) and its damage severity (reduction in axial stiffness of each member). Then, the FRF data are compressed (stage 2). Large size of the FRF data is very problematic in damage detection of truss bridges with high degrees of freedom (i.e. large number of members), as it requires very large space, high data generation, and training time. Thus, PCA is applied to the FRF data sets to determine the principal components of the data. Data compression also increases the performance of the CSC algorithm by removal of multi-collinearity. Afterwards, some part of the compressed data set is used in the CSC algorithm to create a damage model of the bridge, named as training data set (stage 3). It basically creates a relationship between the FRF data and the damage data. Once the damage model of the bridge is generated (stage 4), the remaining part of the FRF data, named as testing FRF data (stage 5), is used to predict the damage severity and location (stage 6). The actual damage data is used to determine the accuracy of the damage model. In following section, the formulation of FRFs, data compression, and CSC algorithm are mathematically presented in detail.

2.1 Frequency Response Functions

The equation of motion for a truss bridge with *n* degrees of freedom (DOFs) is given by:

$$\mathbf{M}\ddot{\mathbf{x}}(t) + \mathbf{C}\dot{\mathbf{x}}(t) + \mathbf{K}\mathbf{x}(t) = \mathbf{F}(t) \qquad (1)$$

where **M**, **C**, and **K** are $n \times n$ global mass, damping, and stiffness matrices, respectively. If we consider a harmonic excitation, the external force, **f**, and displacement, **x**, vectors are given by:

$$\mathbf{f}(t) = \mathbf{F}(\omega)\mathrm{e}^{i\omega t} \qquad (2a)$$

and,

$$\mathbf{x}(t) = \mathbf{X}(\omega)\mathrm{e}^{i\omega t} \qquad (2b)$$

Substituting equations (2a) and (2b) into equation (1) gives:

$$\left(-\omega^2\mathbf{M} + i\omega\mathbf{C} + \mathbf{K}\right)\mathbf{X}(\omega)\mathrm{e}^{i\omega t} = \mathbf{F}(\omega)\mathrm{e}^{i\omega t} \qquad (3)$$

and subsequently, the FRF matrix, $\mathbf{H}(\omega)$ is given by:

$$\mathbf{H}(\omega) = \left(-\omega^2\mathbf{M} + i\omega\mathbf{C} + \mathbf{K}\right)^{-1} \qquad (4)$$

The number of the FRFs to be used for damage detection purposes depends on the number of excitations, and vibration response measurements for a truss bridge.

2.2 Data Compression

Principal Component Analysis (PCA) is used in this study to reduce the size of the FRF data (Jolliffe, 1986; Bishop, 1995). It transforms the original FRF data set of correlated variables in an *N*-dimensional space into a new set of uncorrelated variables called Principal Components (PCs), in a *P*-dimensional space ($P < N$) through an orthogonal projection (Zang and Imregun., 2001). Using all available FRF data of the damaged bridge, FRF matrix, $\mathbf{H}(\omega)_{M\times N}$, is formed where *M* is the number of FRFs, and *N* is the number of frequency points. The mean of the *j*th column of the FRF data is expressed as:

Accepted manuscript doi: 10.1680/jbren.22.00017

$$\overline{H}_j(\omega) = \frac{1}{M}\sum_{i=1}^{M} H_{ij}(\omega) \qquad (5)$$

and, the corresponding standard deviation, S_j, is defined as:

$$S_j^2 = \frac{1}{M}\sum_{i=1}^{M} (H_{ij}(\omega) - \overline{H}_j(\omega))^2 \qquad (6)$$

where $H_{ij}(\omega)$ is an element of the FRF matrix, and is replaced by:

$$H_{ij}(\omega) = \frac{H_{ij}(\omega) - \overline{H}_j}{S_j\sqrt{M}} \qquad (7)$$

and, the correlation matrix is given by:

$$\mathbf{D}_{N\times N} = \mathbf{H}^T_{N\times M}\,\mathbf{H}_{M\times N} \qquad (8)$$

where $\tilde{\mathbf{H}}(\omega)$ is the variation matrix, and its *ij*th element is $H_{ij}(\omega)$. Thus, the *i*th PC, $\boldsymbol{\phi}_i$, is given by:

$$\mathbf{D}\boldsymbol{\phi}_i = \lambda_i\boldsymbol{\phi}_i \qquad (9)$$

The projection of the variation matrix, $\tilde{\mathbf{H}}(\omega)$, on the *N* principal components is given by:

$$\mathbf{A} = \tilde{\mathbf{H}}(\omega)\boldsymbol{\Psi} \qquad (10)$$

where $\boldsymbol{\Psi} = [\boldsymbol{\phi}_1 \quad \ldots \quad \boldsymbol{\phi}_N]$. Afterwards, the variation matrix is reconstructed for the first *P* PCs, and the remaining PCs, *N*-*P*, are eliminated:

$$\tilde{\mathbf{H}}_R(\omega) = \mathbf{A}_{M\times P}\boldsymbol{\Psi}^T_{P\times N} \qquad (11)$$

Finally, the elements of the compressed FRF data, $H_{ij}(\omega)$, is reconstructed using the elements of the reconstructed variation matrix, $\tilde{\mathbf{H}}_R(\omega)$, in equation (7).

2.3 Formulation of CSC Algorithm

Recently, Sparse Representation (SR) of data has received much attention in pattern recognition and machine learning community as a robust tool for representing noisy signals (Wright et al., 2009). Sparsity means that a signal can be sufficiently described using a few active features without loss of information. Within the context of the current study, the *j*th compressed FRF data, $\mathbf{H}_j$, of length *P*, is represented as a sparse linear combination:

$$\begin{aligned} &\mathbf{H}_j \approx \mathbf{D}_H\boldsymbol{\alpha} \\ &\boldsymbol{\alpha} = [\alpha_1 \quad \alpha_2 \quad \ldots \quad \alpha_i \quad \ldots. \quad \alpha_K]^{\mathrm{T}} \end{aligned} \qquad (12)$$

where $\boldsymbol{\alpha}$ has K elements and is the sparse code of the jth FRF data, H_j; $\mathbf{D}_H$ is a transformation matrix of size $P \times K$, and is the dictionary of the the jth FRF data. In a similar approach, the jth damage data is represented by:

$$\mathbf{Y}_j \approx \mathbf{D}_{\mathrm{Y}} \boldsymbol{\alpha} \qquad (13)$$

in which, $\mathbf{D}_{\mathrm{Y}}$ is a transformation matrix of size $Q \times K$, and is the dictionary of the jth damage data. Generally, CSC uses $\mathbf{H}_j$ and $\mathbf{Y}_j$ as inputs, establish a relationship between the damage feature and the damage information for the truss bridge through an optimization problem:

$$\min_{\alpha \in R^K} : \left\| \mathbf{H}_j - \mathbf{D}_{\mathrm{X}} \boldsymbol{\alpha} \right\|_2^2 + \kappa_1 \left\| \boldsymbol{\alpha} \right\|_1 + \kappa_2 \left\| \mathbf{Y}_j - \mathbf{D}_{\mathrm{Y}} \boldsymbol{\alpha} \right\|_2^2 \qquad (14)$$

where κ_1 and κ_2 are called the regularization parameters; $\| \ \|_1$ and $\| \ \|_2$ are the first and second norm operators, respectively. The test FRF data, $\mathbf{H}'_j$, is then used in the trained model (equation (14)), to estimate the damage, Y'_j:

$$\min_{\mathrm{Y}'_j \in R^{M \times P}} : \left\| \mathbf{H}'_{j\,j} - \mathbf{D}_{\mathrm{X}} \alpha \right\|_2^2 + \kappa_1 \left\| \alpha \right\|_1 + \kappa_2 \left\| \mathrm{Y}'_j - \mathbf{D}_{\mathrm{Y}} \alpha \right\|_2^2 \qquad (15)$$

The feature-sign search algorithm is used to solve the optimization problems in equations (14) and (15), (Lee et al., 2007).

3. Application of the Proposed Method

To demonstrate the efficiency and performance of the proposed method in damage detection of truss bridges, two truss bridges are studied. For each truss bridge, the FRF data of the damaged structures are created through reliable Finite Element (FE) models. In this study, FE model of each bridge is constructed using MATLAB. To model each truss bridge in MATLAB, global stiffness, mass, and damping matrices need to be created (see equation (1)). The local axial stiffness matrix of each member are first formed, then transformed to assemble the global stiffness matrix of the truss bridge. The mass of each member is distributed over its nodes as lumped masses, and then the global mass matrix is constructed. The global damping matrix is determined using Rayleigh damping concept, which is a combination of global stiffness and mass matrices. Finally, to create FRFs for each bridge, single harmonic excitation is applied at the vertical DOFs of a number of nodes, and vibration response of horizontal and vertical DOFs of some nodes are determined using Newmark-Beta

Accepted manuscript doi:
10.1680/jbren.22.00017

integration scheme. The nodes are selected based on practical health monitoring in truss bridges. It is assumed that the vibration exciter can excite the bridge in the frequency range of 0-300 Hz, and the vibration response data are completely generated. This frequency range was obtained based on a sensitivity analysis, and could be different for different structures. The vibration-to-excitation ratio of the bridge over the frequency range gives the FRF data. Figure 2 shows an exemplar FRF over frequency range of 0 to 300 Hz. In some studies, the frequency range of the FRFs is selected based on the resonance and anti-resonance regions (Nozarian and Esfandiari, 2009; Ni et al., 2006; Lee and Shin, 2002; Shadan et al., 2015). This causes a significant data loss which could result in inaccuracies and poor resolution of the damage detection technique. Thus, in this study, the entire frequency range of the FRF data (0-300 Hz) is used. A random white Gaussian noise with zero mean and unit standard deviation is added to the FRFs with 5%, 10%, 15%, and 20% levels. This is done to measure the ability of the proposed detection method in differentiating between the actual damage and the noise. The modulus of elasticity, Poisson's ratio, and density of each steel member of truss bridges are taken 200 GPa, 0.3, and 7850 kg/m^3, respectively.

The damage is induced in each model through reduction of axial stiffness of the truss members. Thus, the damage data contains member number and their corresponding stiffness reduction. Then, the training FRF data and corresponding damage data are inputted into the CSC algorithm to create a damage model of each truss bridge. Finally, the testing FRF data are used in the CSC-based damage model to predict the damage (stiffness reduction) of each member of the truss bridges, and the actual testing damage data is used to evaluate the performance of the predicted damage. As stated in the proposed detection algorithm, the PCA method is used to reduce the size of the FRFs and increase computational efficiency.

Figure 3 shows a 25-member truss bridge. It is composed of 6 bays, 12 nodes, and 21 DOFs. Single harmonic excitation is applied at three vertical DOFs of nodes 2, 3 and 10. Horizontal DOFs of nodes 9 and 6 and vertical DOF of node 3 are selected to determine vibration response of the bridge. Since three vibration response DOFs and three excitation DOFs have been selected, the FRF data includes 9 sets of FRFs. Figure 4 shows the second truss bridge with 9 bays, 40 member, 18 nodes, and 33 DOFs. Excitation are applied at vertical DOFs of nodes no. 2, 5 and 7 and vibration response of the bridge is determined at horizontal DOFs of nodes 4, 17 and 10. Table 1 summarizes various single and multiple damages scenarios considered for both bridges.

Figures 5 and 6 compare the predicted and actual damages for different damage scenarios of the both bridges in presence of 20% noise. As seen in both figures, the proposed method reliably predicts the damage severity, and also the location of the damage (member no.) is accurately determined. Figure 7 illustrates the damage detection results of the 40-member bridge for various noise levels. As seen, the performance of the proposed method is reliable even in the presence of high levels of noise (20%).

To better quantify the effects of various noise levels, the mean correct classification rate was used to determine the accuracy of the proposed method for 100 multiple damage scenarios. Table 2 and 3 summarize the accuracy of the proposed method to identify damage location and severity of both bridges for various noise levels. 1. As seen in Tables 2 and 3, with the increase of the noise level, the accuracy appears to reduce (up to around 5% reduction for 20% noise level with respect to the noise free data, 0%). However, even in the case of the 20% noise level, the accuracy of the proposed method is over 90% in both damage location and severity for both bridges. Thus, the increase of the noise level does not significantly affect the method's accuracy.

For the 25-member bridge, a full set of FRFs contains 10800 data points over a frequency range of 0-300 Hz (frequency increment of 0.25 Hz). This corresponds to 6750 input nodes for the CSC algorithm. Such a large number of input nodes may diminish training convergence as well as computational efficiency. Hence, PCA reduces this dimension (6750) to 20, 50, 100 and 200 PCs.

1. Conclusion

This work addresses the application of Couple Sparse Coding (CSC) algorithm as a powerful pattern recognition model in smart damage detection of truss bridges in the presence of high levels of measurement noise. For this purpose, the FRF data are created for reliable FE models and the Principal Component Analysis (PCA) is carried out to compress FRF data. The CSC algorithm is used to estimate damage severity and location of two exemplary truss bridges.

It is found that the CSC algorithm accurately predicts damage location and severity of truss bridges even in the presence of high levels of noise. Further, it is seen that the accuracy of the proposed method in damage localization does not depend on the number of PCs. Generally, the method successfully improves the accuracy of structural damage localization in the presence of high levels of measurement noise and incomplete FRF data in truss bridges.

Additionally, the method has a great potential to be implemented in vibration-based damage detection of real-life truss bridges. With the use of the CSC algorithm, some critical obstacles of traditional damage identification techniques, such as over-fitting in large-DOF structures and high-level noise can be overcome, and damage detection accuracy and reliability can be significantly improved.

Notation

$\mathbf{A}$	Projection matrix of the principal components
$\mathbf{C}$	Global damping matrix
$\mathbf{D}$	Correlation matrix
$\mathbf{D}_H$	The transformation matrix or dictionary for frequency response function matrix
$\mathbf{D}_Y$	The transformation matrix or dictionary for damage matrix
$\mathbf{F}(\omega)$	External force in frequency domain
$\mathbf{f}(t)$	External force in time domain
$\mathbf{H}$	Frequency response function matrix
$\tilde{\mathbf{H}}$	Variation matrix
$\tilde{\mathbf{H}}_R$	The reconstructed frequency response function matrix
$\mathbf{H}'_j$	The *j*th test frequency response function
H_{kj}	The *kj*th element of the frequency response function
$\overline{H}_j$	The mean of the *j*th column of the frequency response function matrix
H_{kj}	The *kj*th element of the variation matrix
i	The imaginary unit of a complex number
$\mathbf{K}$	Global stiffness matrix
$\mathbf{M}$	Global mass matrix
M	Number of frequency response functions
N	Number of frequency points
n	Number of degrees of freedom
S_j	The standard deviation corresponding to the *j*th column of the frequency response function matrix
T	Transpose of a matrix
t	Time
$\mathbf{X}$	Displacement vector in frequency domain
$\mathbf{x}(t)$	Displacement vector in time domain
$\dot{\mathbf{x}}(t)$	Velocity vector in time domain
$\ddot{\mathbf{x}}(t)$	Acceleration vector in time domain
$\mathbf{Y}$	Damage matrix
$\mathbf{Y}'$	The *j*th test damage data
$\boldsymbol{\alpha}$	Sparse vector for the *j*th frequency response function

λ_k	The *k*th Eigen value corresponding to the *k*th principal component
$\boldsymbol{\phi}_k$	The *k*th principal component
$\boldsymbol{\Psi}$	Matrix of all principal components
ω	Circular frequency

References

A.Perez-Ramirez C, P.Amezquita-Sanchez J, Adeli H, et al. (2016) New Methodology for Modal Parameters Identification of Smart Civil Structures using Ambient Vibrations and Synchrosqueezed Wavelet. *Engineering Applications of Artificial Intelligence* 48: 1-16.

Alexandrino PdSL, Gomes GF and Cunha Jr SS (2020) A robust optimization for damage detection using multiobjective genetic algorithm, neural network and fuzzy decision making. *Inverse Problems in Science and Engineering* 28(1): 21-46.

Avci O, Abdeljaber O, Kiranyaz S, et al. (2018) Wireless and real-time structural damage detection: A novel decentralized method for wireless sensor networks. *Journal of sound and vibration* 424: 158-172.

Avci O, Abdeljaber O, Kiranyaz S, et al. (2020) Structural health monitoring with self-organizing maps and artificial neural networks. *Topics in Modal Analysis & Testing, Volume 8*. Springer, pp.237-246.

Bandara RP, Chan TH and Thambiratnam DP (2014) Frequency response function based damage identification using principal component analysis and pattern recognition technique. *Engineering Structures* 66(1): 116-128.

Bishop C (1995) *Neural Networks for Pattern Recognition.*

Bokaeian V, Khoshnoudian F and Fallahian M (2021) Structural damage detection in plates using a deep neural network–couple sparse coding classification ensemble method. *Journal of Vibration and Control* 27(3-4): 437-450.

Dackermann U, Li J and Samali B (2013) Identification of member connectivity and mass changes on a two-storey framed structure using frequency response functions and artificial neural networks. *Journal of sound and vibration* 332(16): 3636-3653.

Doebling SW, Farrar CR and Prime MB (1998) A summary review of vibration-based damage identification methods. *Shock and vibration digest* 30(2): 91-105.

Fallahian M, Ahmadi E and Khoshnoudian F (2022) A structural damage detection algorithm based on discrete wavelet transform and ensemble pattern recognition models. *Journal of Civil Structural Health Monitoring* 12(2): 323-338.

Fallahian M, Khoshnoudian F and Talaei S (2018a) Application of couple sparse coding ensemble on structural damage detection.

Fallahian M, Khoshnoudian F, Talaei S, et al. (2018b) Experimental validation of a deep neural network—Sparse representation classification ensemble method. *The Structural Design of Tall and Special Buildings* 27(15).

Fang X, Luob H and Tang J (2005) Structural damage detection using neural network with learning rate improvement. *Computers & Structures* 83(25-26): 2150-2161.

Furukawa A, Otsuka H and Kiyono J (2006) Structural damage detection method using uncertain frequency response functions. *Computer-Aided Civil and Infrastructure Engineering* 21(4): 292-305.

Hwang HY and Kim C (2004) Damage detection in structures using a few frequency response measurements. *Journal of sound and vibration* 270(1): 1-14.

J.A. Pereira, W. Heylen, S. Lammens, et al. (1995) Influence of the number of frequency points and resonance frequencies on model updating techniques for health condition monitoring and damage detection of flexible structure. *Proceedings of the 13th International Modal Analysis Conference.* Nashville, 1273–1281.

Jolliffe IT (1986) *Principal Component Analysis.*

Lee U and Shin JA (2002) A frequency response function-based structural damage identification method. *Computers & structures* 80(2): 117–132.

Li J, Dackermann, U., Xu YL and Samali B (2012) Damage identification in civil engineering structures utilizing PCA-compressed residual frequency response functions and neural network ensembles. *Structural Control and Health Monitoring* 18(2): 207-226.

Li Y and Fang. Y (2012) T-S neural network model identification of ultra-supercritical units for superheater based on improved fcm. *Research Journal of Applied Sciences, Engineering and Technology* 4(14): 2147-2152.

Mehrjoo M, Khaji N, Moharrami H, et al. (2008) Damage detection of truss bridge joints using Artificial Neural Networks. *Expert Systems with Applications* 35(3): 1122-1131.

Ni YQ, Zhou XT and Ko JM (2006) Experimental investigation of seismic damage identification using PCA-compressed frequency response functions and neural networks. *Journal of sound and vibration* 290(1): 242-263.

Nozarian MM and Esfandiari A (2009) Structural damage identification using frequency response function. *Materials forum* 33: 443-449.

Padil KH, Bakhary N, Abdulkareem M, et al. (2020) Non-probabilistic method to consider uncertainties in frequency response function for vibration-based damage detection using artificial neural network. *Journal of sound and vibration* 467: 115069.

Rumelhart DE, Williams. RJ and Hinton. GE (1986) Learning representations by back-propagating errors. *Nature* 323: 533 - 536.

Shadan F, Khoshnoudian F and Esfandiari A (2015) A frequency response-based structural damage identification using model updating method. *Structural Control and Health Monitoring* DOI: 10.1002/stc.1768.

Tan ZX, Thambiratnam DP, Chan TH, et al. (2020) Damage detection in steel-concrete composite bridge using vibration characteristics and artificial neural network. *Structure and Infrastructure Engineering* 16(9): 1247-1261.

Wright J, Ma Y, Mairal J, et al. (2009) Sparse representation for computer vision and pattern recognition *Proceedings of the IEEE* 98(6).

Xu B, Wu, Z., Chen G and Yokoyama K (2004) Direct identification of structural parameters from dynamic responses with neural networks. *Engineering Applications of Artificial Intelligence* 17(8): 931-943.

Accepted manuscript doi: 10.1680/jbren.22.00017

Yu Y, Wang C, Gu X, et al. (2019) A novel deep learning-based method for damage identification of smart building structures. *Structural Health Monitoring* 18(1): 143-163.

Zang C and Imregun. M (2001) Structural damage detection using artificial neural networks and measured FRF data reduced via principal component projection. *Journal of Sound and Vibration* 242(5): 813-827.

Zenzen R, Khatir S, Belaidi I, et al. (2020) A modified transmissibility indicator and Artificial Neural Network for damage identification and quantification in laminated composite structures. *Composite Structures* 248: 112497.

Zhao R, Yan R, Chen Z, et al. (2019) Deep learning and its applications to machine health monitoring. *Mechanical systems and signal processing* 115: 213-237.

Zolfaghari M, Jourabloo A, S G, et al. (2014) 3D human pose estimation from image using couple sparse coding. *Machine Vision & Applications* 25(6): 1489.

Table 1. Damage scenarios for 25- and 40-member bridges.

Bridges	Damage Scenarios	Element No.	Actual Damage (%)
25-member Bridge	Case1	5	50
	Case2	6	11
		18	5
	Case3	7	40
		12	50
		23	45
	Case4	4	20
		10	25
		18	20
		23	20
40-member Bridge	Case1	14	35
	Case2	14	50
		18	60
	Case3	7	10
		35	15
		38	10
	Case4	10	30
		18	35
		23	25
		28	30

Table 2. Accuracy of the damage detection results for the 25-member bridge in the presence of various noise levels

Noise Level	0%	5%	10%	15%	20%
Damage Location Estimation (%)	99.23	98.15	96.86	96.02	95.53
Damage Severity Estimation (%)	99.04	97.21	95.98	95.20	94.37

Accepted manuscript doi:
10.1680/jbren.22.00017

Table 3. Accuracy of the damage detection results for the 40-member bridge in the presence of various noise levels

Noise Level	0%	5%	10%	15%	20%
Damage Location Estimation (%)	98.12	96.50	95.95	95.64	94.75
Damage Severity Estimation (%)	97.53	97.05	95.50	94.14	92.63

Figure captions

Figure 1. Proposed algorithm for damage detection of truss bridges

Figure 2. An exemplar frequency response function.

Figure 3. Truss bridge with 25 members: (a) geometry of the bridge (node numbers are in red and element numbers are in blue), and (b) DOFs of all nodes.

Figure 4. Truss bridge with 40 members: (a) geometry of the bridge (node numbers are in red and element numbers are in blue), and (b) DOFs of all nodes.

Figure 5. Damage detection results of the 25-member truss bridge for damage scenario: (a) 1, (b) 2, (c) 3, and (d) 4.

Figure 6. Damage detection results of the 40-member truss bridge for damage scenario: (a) 1, (b) 2, (c) 3, and (d) 4.

Figure 7. Damage detection results of the 40-member truss bridge for various levels of noise.

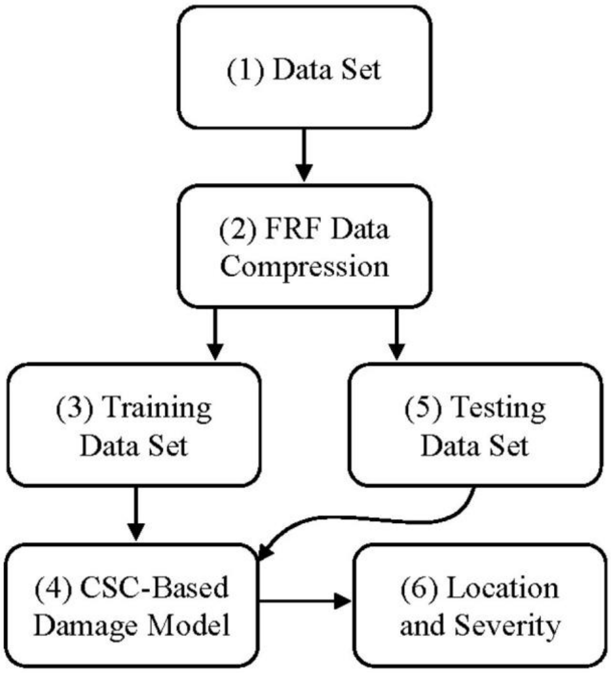
(1) Data Set
(2) FRF Data Compression
(3) Training Data Set
(5) Testing Data Set
(4) CSC-Based Damage Model
(6) Location and Severity

Figure 1

Accepted manuscript doi:
10.1680/jbren.22.00017

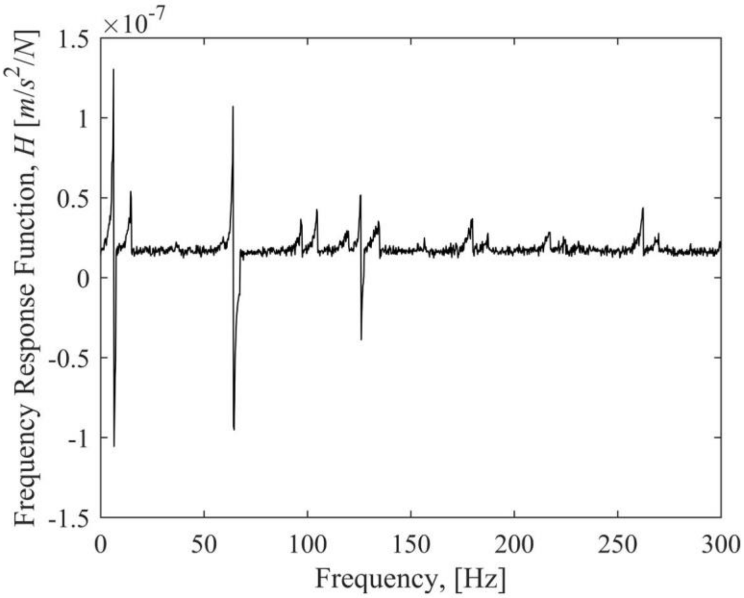

Figure 2

Accepted manuscript doi:
10.1680/jbren.22.00017

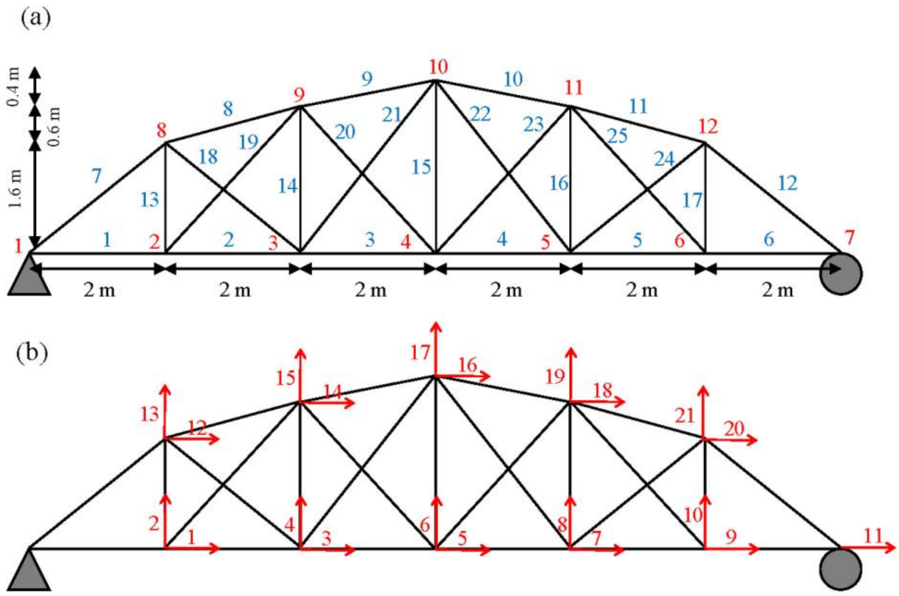

Figure 3

Accepted manuscript doi:
10.1680/jbren.22.00017

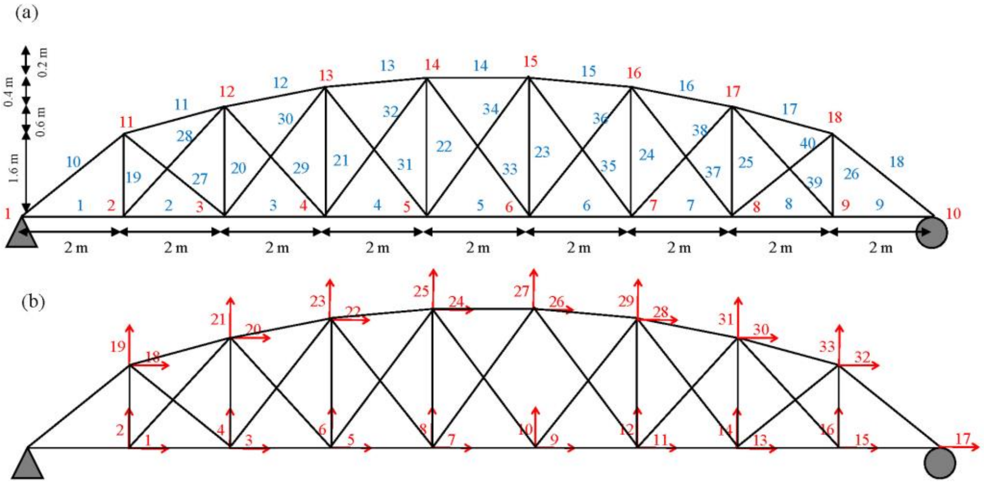

Figure 4

Accepted manuscript doi:
10.1680/jbren.22.00017

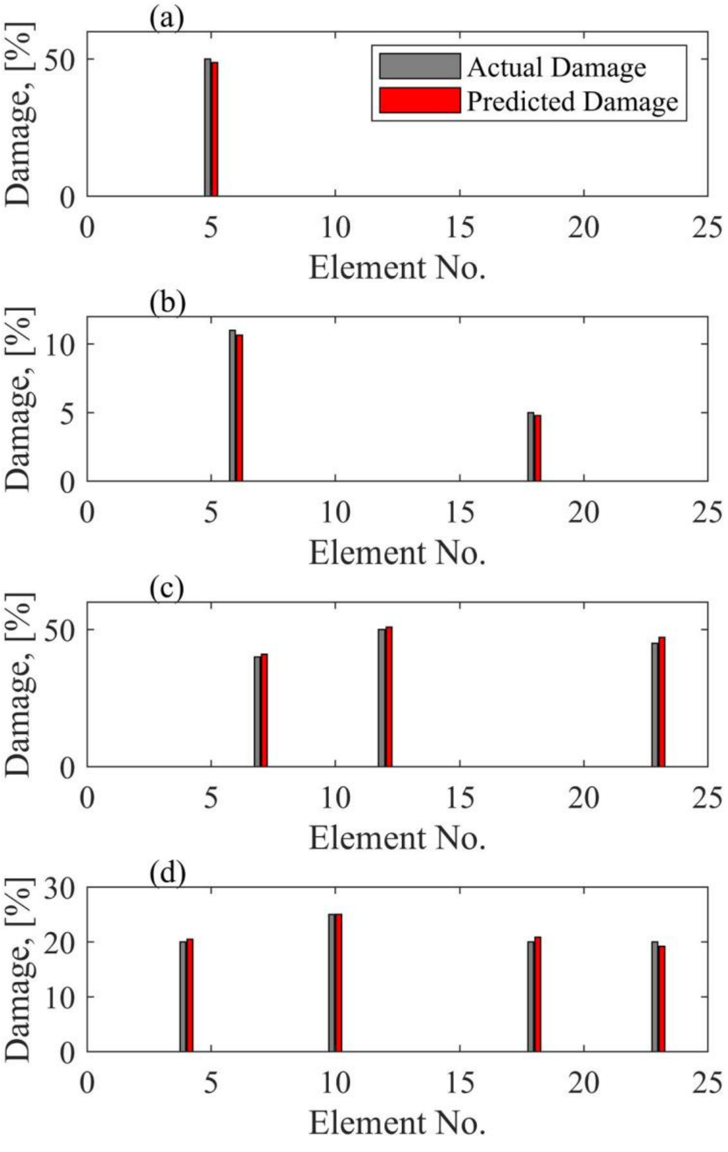

Figure 5

Accepted manuscript doi:
10.1680/jbren.22.00017

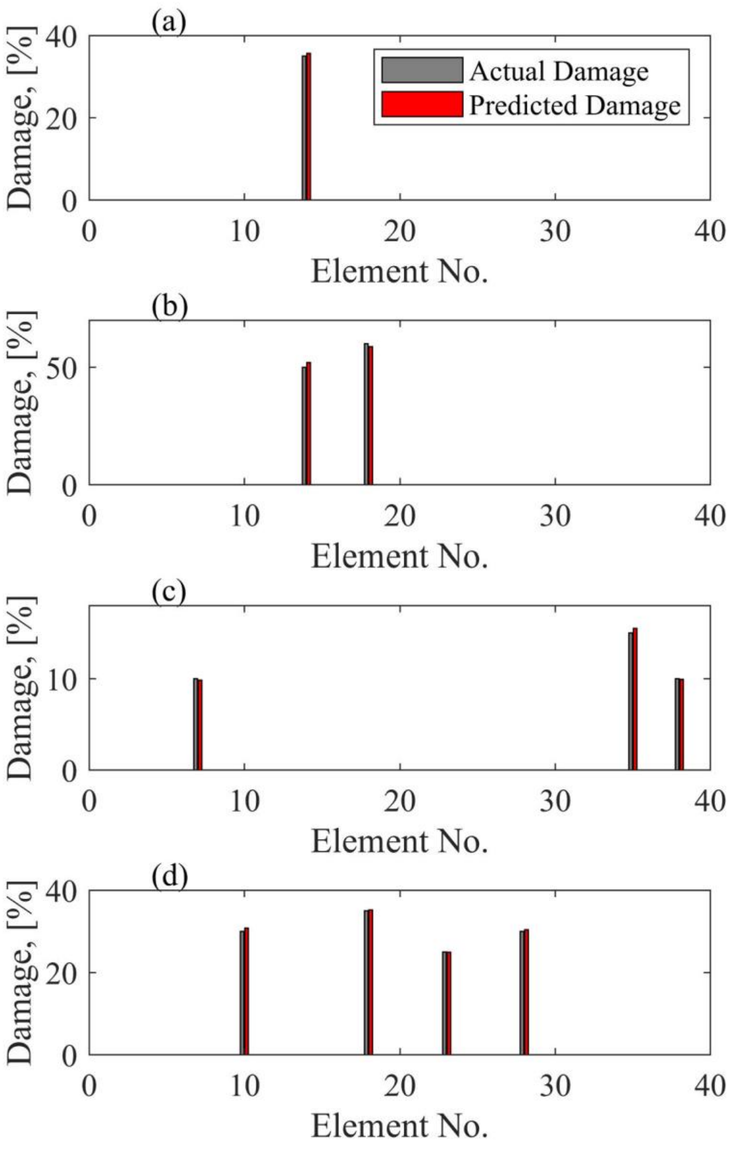

Figure 6

Accepted manuscript doi:
10.1680/jbren.22.00017

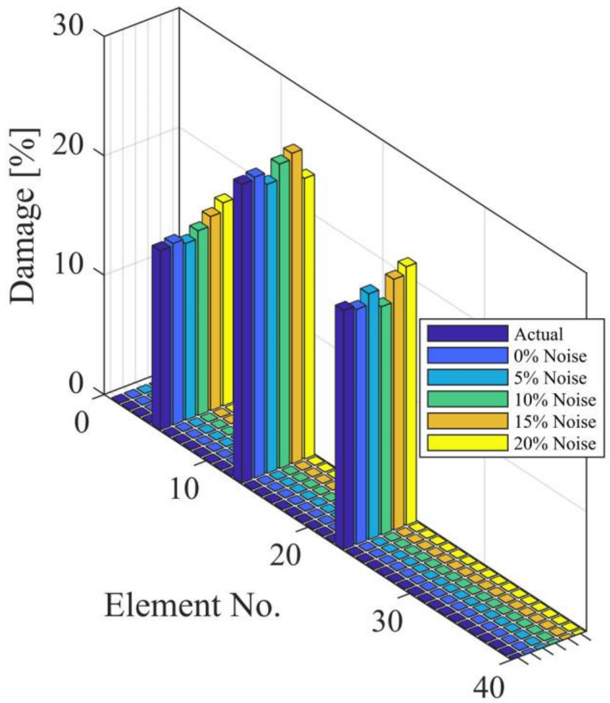

Figure 7